16TH EUROPEAN CONFERENCE ON EARTHQUAKE ENGINEERING THESSALONIKI 18 - 21 JUNE 2018

SEISMICALLY-INDUCED STRAIN EFFECTS IN HIGHLY HETEROGENEOUS DEPOSITS: THE FOSSO DI VALLERANO ALLUVIAL VALLEY (ROME, ITALY)

Céline BOURDEAU[1], Luca LENTI[1], Salvatore MARTINO[2], Chiara VARONE[3*]

ABSTRACT

The Fosso di Vallerano alluvial valley (Rome, Italy) was selected to evaluate earthquake–induced effects in highly heterogeneous deposits. A high-resolution engineering-geological model was derived from field investigations, technical reports and geophysical surveys. Based on this engineering-geological model, 4 main lithotechnical units were distinguished: i) Plio-Pleistocene marine deposits; ii) Pleistocene alluvial deposits of the Paleo Tiber 4 River; iii) volcanic deposits of the Alban Hills and of the Monti Sabatini Volcanic Districts; iv) recent alluvial deposits that filled the valley incisions since the end of the Würmian regression. 1D and 2D numerical modelling were carried out to analyse induced strain effects within the alluvial deposits by assuming a non-linear behaviour of all materials under free-field conditions (i.e. absence of structures). Strong motion time-histories were applied at the seismic bedrock and earthquake-induced strains were computed in terms of maximum shear strain (MSS) adopting different assumptions: i) 1D conditions, ii) 2D conditions, iii) homogeneous filling (i.e. with properties representative of the main resonance frequencies of the valley: ≈ 0.8 Hz), iv) highly heterogeneous filling. These simulations allowed evaluating the Shear Strain Concentration Index (SSCI) in 1D as well as in 2D conditions for each lithological unit. The computed SSCI values highlight concentrations of shear strain in the engineering-geological model as well as the role of 2D effects in the distribution of shear strain within the alluvial deposits.

Keywords: Highly heterogeneous deposits; Non-linear behavior; Numerical modeling; Rome.

1. INTRODUCTION

This paper focuses on the evaluation of earthquake–induced effects in highly heterogeneous deposits through a numerical approach. The Fosso di Vallerano (Rome, Italy) alluvial valley was selected as case study according to its highly heterogeneous geological setting. A detailed engineering-geological model of the valley was reconstructed based on available field investigation results as well as technical reports (Bozzano et al. 2016). The seismo-stratigraphic setting of the alluvial body was initially calibrated trough a 1D numerical modelling (Bozzano et al. 2016; Varone et al. 2014) and the obtained dynamic properties of the local seismo-stratigraphy were applied to corresponding lithological units in the entire valley; in the following, 2D numerical modelling was carried out to analyse the local seismic response and the strain effects induced within the alluvial deposits by assuming non-linear behaviour of the deposits. This paper discusses some results focused on the earthquake-induced strain effects using specific indexes for quantifying shear-strain concentrations and distributions within the alluvial deposits (Martino et al., 2015).

[1]University Paris-Est LCPC/ The French institute of science and technology for transport, development and networks (IFSTTAR) / Department GERS-14-20 Boulevard Newton Cité Descartes, Champs-sur-Marne F-77447 Marne–la-Vallée Cedex 2, France. celine.bourdeau@ifsttar.fr , luca.lenti@ifsttar.fr
[2]Department of Earth Sciences of the University of Rome «Sapienza» and Research Center for the Geological Risks (CERI). P.za A. Moro 5 00185 Rome, Italy. salvatore.martino@uniroma1.it
[3] École Supérieure d'Ingénieurs des Travaux de la Construction (ESITC) de Paris - 79, Avenue Aristide Briand, 94110, Arcueil, France. chiara.varone@esitc-paris.fr

2. ENGINEERING - GEOLOGICAL SETTING

The Fosso di Vallerano valley (Fig. 1) is located in the southern part of Rome and it includes two secondary valleys which join before the confluence of the Vallerano and the Cecchignola creeks in the Tiber River. The Fosso di Vallerano valley is characterized by a flat portion that corresponds to flood plains (10 m a.s.l.) that are bordered by hills (35-50 m a.s.l.). The area also exhibits a complex geomorphological setting inherited from the Würmian glacio-eustatic cycle, which led to a series of successive deviations and rearrangements of the river bed (Ascani et al. 2008).

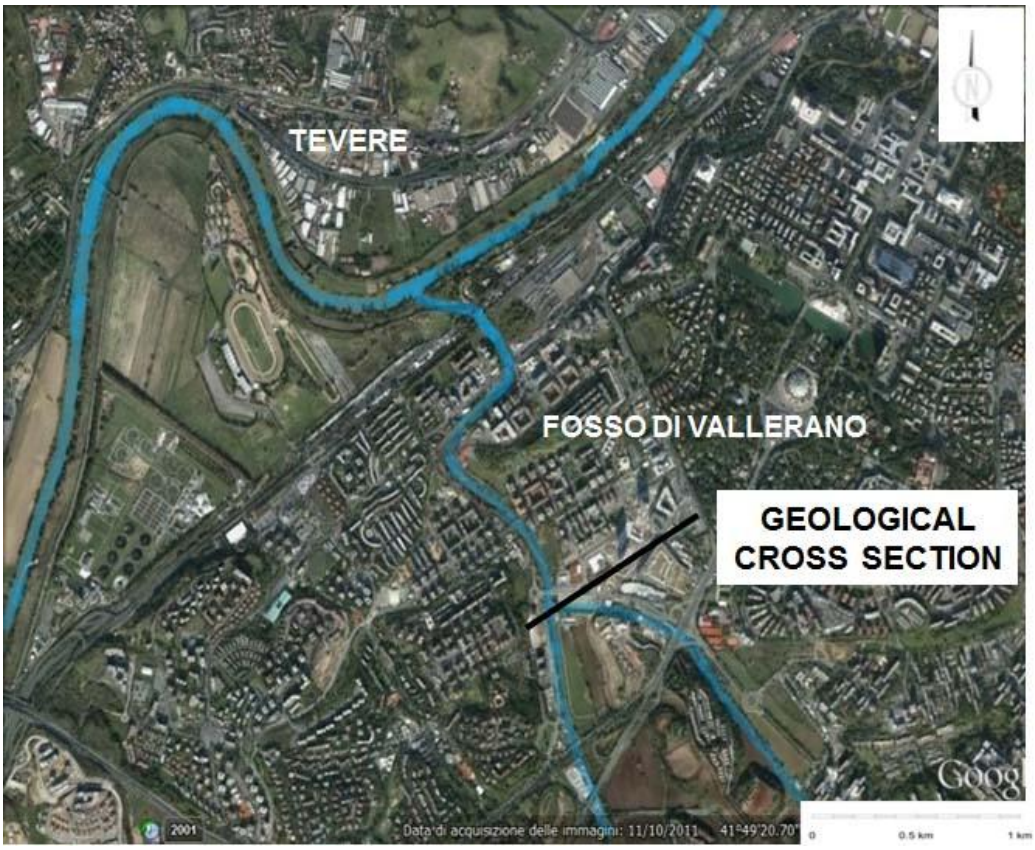

Figure 1. – Satellite view of the Fosso di Vallerano valley.
The track of the geological cross-sections considered in this study is also reported.

According to Bozzano et al. (2016), the subsoil geology of the Fosso di Vallerano valley includes 4 lithological units: 1) Plio-Pleistocene marine deposits (Marne Vaticane Formation) consisting in high consistency clays with silty-sandy levels (PP); 2) Pleistocene alluvial deposits of the Paleo Tiber 4 River (650-600 ky) consisting in gravels, sands and clays (PT); 3) volcanic deposits of the Alban Hills and of the Monti Sabatini Volcanic Districts (561-360 ky) consisting of highly heterogeneous tuffs (VL) ; 4) recent alluvial deposits that filled the valley incisions since the end of the Würmian regression (18 ky-Present), characterized by a basal gravel level and including different soft soils from sands to inorganic or peaty clays (AL). The Plio-Pleistocene marine deposits represent the local geological bedrock while the local seismic bedrock (Vs $\geq$ 800 m/s) is located at the top of the Pleistocene gravels (Paleo Tiber 4 deposits). The description of the geological setting of the area and the geophysical data derived from field surveys were used to provide a high-resolution engineering-geological model of the valley. The dynamic properties attributed to the subsoils of the Fosso di Vallerano valley are reported in Table 1.

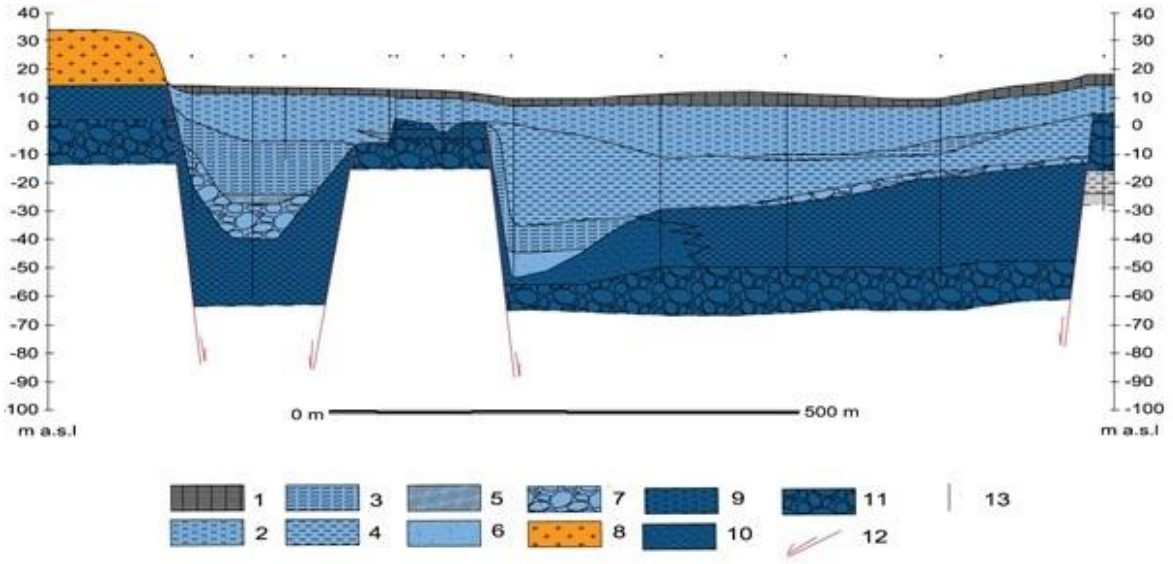

Figure 2. Geological cross section considered in this paper. Legend: AL deposits: from 1 to 7. VL deposits: 8. PT deposits: from 9 to 11. 12) Fault. 13) Borehole (modified from Bozzano et al. 2016). Refer to Table 1 below for further explanations on the various lithologies composing the cross section.

Table 1. Dynamic properties attributed to the lithological units characterizing the cross section shown in Fig. 2. (Modified from Bozzano et al. 2016). In the Table γ is the weight per unit volume, G0 is the maximum shear modulus and γ_{ref} is the strain at which the modulus-reduction curve cross the G/G0 = 0.5 (see § 3 for more information).

	Lithology	**γ (kN/m^3)**	**G_0 (MPa)**	**Vs (m/s)**	**γ_{ref} (%)**
Alluvial Body - AL	1 Anthropic fill material	17	82	118	0.008
	2 Volcano- clastic sandy clays	16.5	53	**225**	0.020
	3 Peaty clays	17.2	64	**150**	0.150
	4 Silty clays	18.3	66	235	0.150
	5 Peat	12.7	25	140	0.050
	6 Sands	19.2	334	417	0.008
	7 Gravel	21.0	1068	713	0.008
Volcanic deposit - VL	8 Tuffs	21.0	1068	800	0.008
Paleo-Tiber Deposits - PT	9 Silty clays	18.3	101	**357**	0.150
	10 Sands	19.2	334	417	0.008
	11 Gravel	21.0	1068	1100	0.008

3. NUMERICAL MODELLING SETTING

Numerical simulations were performed along the geological cross section shown in Fig. 2 using some of the strong motions provided by the Italian Technical Rule (D.G.R. Lazio 387/09) as inputs at the seismic bedrock level. These strong motions are characterized by a constant PGA equal to 0.168 g, an Arias Intensity varying between 0.06 m/s^2 and 0.2 m/s^2 and frequency content in the range 0 – 15Hz. The 1D numerical modelling was done through the EERA code (Equivalent – linear Earthquake Response Analysis, Bardet et al. (2000)) by discretizing the domain into 56 soil columns with a lateral representativeness of 10 m while the 2D numerical simulations were done using the 2D finite difference code FLAC 7.0 (Itasca, 2011).
In addition, 1D and 2D numerical simulations were also performed assuming a homogeneous alluvial filling (Lithological unit 4) to shed light on the impact of 2D effects on the seismic response of the site (Martino et al., 2015 and references therein).
The 2D numerical models were designed following the guidelines of Itasca codes (Itasca, 2011) in terms of discretization of the models into quadrilateral zones allowing an accurate representation of wave transmission through the models up to the highest frequency component of the input motions that contain appreciable energy (Kuhlemeyer and Lysmer, 1973).
An element size of 1 m was therefore adopted for the 2D models allowing an accurate representation of wave transmission through the models up to 10 Hz. Absorbing quiet boundaries (Lysmer and Kuhlemeyer, 1969) were applied along the base of the models to prevent the reflection of outward propagating waves back into the models. And free field boundaries (Cundall et al., 1980) were defined along the lateral boundaries of the models in order to achieve free field conditions.

A non-linear rheology was assumed for all the lithological units characterizing the cross section. The decay curves associated to each lithological unit were defined according to Bozzano et al., 2008 and Caserta at al., 2012. It was simulated using one of the built-in hysteretic damping functions of FLAC software, namely the Hardin/Drnevich model (1972) defined by the equation (1):

$$MS = \frac{1}{1+\frac{\gamma}{\gamma ref}} \qquad (1)$$

where Ms is the strain-dependent normalized secant modulus, γ is the shear strain and γ_{ref} is the strain at which the modulus-reduction curve crosses the G/G0 = 0.5 line.
According to FLAC manual (Itasca, 2011), hysteretic damping provides almost no energy dissipation at very low cyclic strain levels, which may be unrealistic. To avoid low-level oscillations, a small amount (between 1 to 3%) of Rayleigh damping was added.
To account for the presence of quiet boundaries along the base of the models (FLAC, 2011), the seismic inputs were applied as shear strains along the seismic bedrock level (i.e., the acceleration and velocity records were transformed into stress records and applied to the quiet boundary).

4. RESULTS

The results were first analyzed in terms of the maximum shear strain (MSS) within each lithological unit along the geological section.

For the 1D conditions, the MSS_{1D} were computed based on the values of shear strains obtained by EERA code.

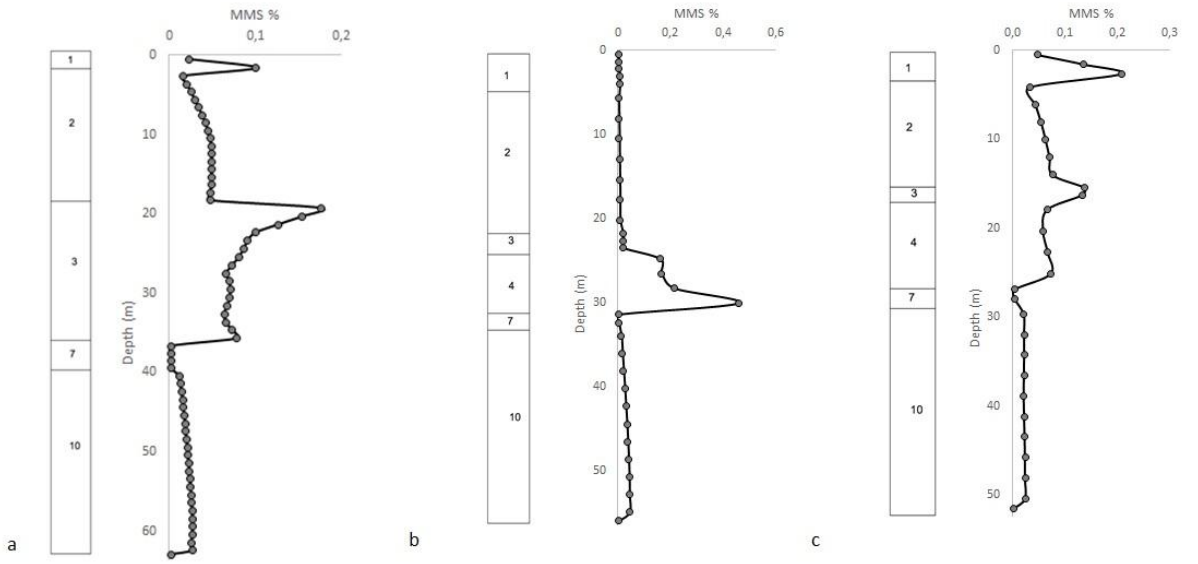

Figure 3. Distributions of the MSS versus depth assuming 1D condition in three of the 56 modelled soil columns. Plots on the left of each MSS curve show the distribution of soil materials along depth for each soil column. Refer to Fig. 2 and Table 1 for the description of the various lithologies.

For the 2D conditions, MSS_{2D} values were obtained along the geological cross section, for each soil column starting from the assessment of the computed displacements using equation (2):

$$MSS_{2D} = \frac{\Delta U}{\Delta H} \tag{2}$$

where ΔU is the difference between the displacements corresponding to two points located at two different depths and at the same distance along the section, ΔH is the difference between the two depths at which displacements are computed.

The analysis of the MMS distribution vs. depth in 1D numerical modelling (Fig. 3) highlighted that the maximum strain value is 0.5 % (middle of Fig.3) while the average value is lower than 0.1%. The higher levels of deformation are achieved in the lithological units 3 or 4. These results are in good agreement with the expected dynamic behavior of the subsoil deposits since they represent the softest lithological units. Besides, it is worth noticing that the strain level of unit 3 in a similar stratigraphic layering (Fig. 5 middle and left), is different according to its position in the soil column. This result is also in good agreement with the ones proposed by Martino et al. (2015) for the main Tiber River valley, corresponding to the historical center of Rome.

The distribution of the MMS vs. depth in case of 2D numerical modelling (Fig. 4) shows results comparable to the ones obtained for the 1D condition. Also in this case, the higher strains are calculated for the lithological units 3 or 4.A significant difference between the seismically induced strain levels achieved in 2D condition with respect to the ones obtained in1D condition, is represented by the maximum strain value (MSV). In 2D condition, the maximum value achieved is 0.3 % while the average is always lower than 0.1%. Also in 2D condition, a different behavior of the lithological unit 3 due to the different stratigraphic position can be observed.

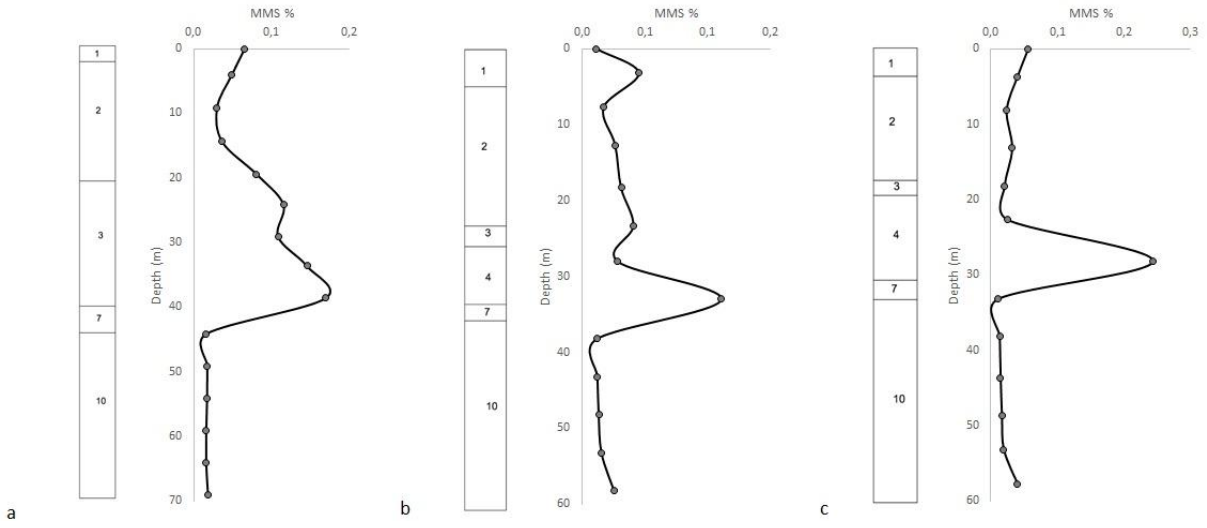

Figure 4. Distribution of the MSS versus depth assuming 2D condition in three of the 56 modelled soil columns.

To filter the role of the stratigraphic position (i.e. depth of the layer in the soil column) the differential indexes proposed by Martino et al. (2015) were computed. For both 1D and 2D conditions, the SSCI (Shear Strain Concentration Index) was also computed (Martino et al., 2015) in order to quantify the MSS concentration within each lithological unit using equation (3):

$$SSCI = \frac{\gamma_{\max} - \gamma_{\min}}{h_{\max} - h_{\min}} \tag{3}$$

in which γ_{max} is the maximum shear strain within each layer in the considered soil column; γ_{min} is the minimum shear strain within each layer in the considered soil column; (h_{max}-h_{min}) is the difference between the two depths at which the minimum and maximum values of the shear strain are obtained.
This index has been computed for each lithological unit assuming a heterogeneous as well as a homogeneous filling of the valley. So the differential index $\Delta\Gamma$ was then computed to subtract the effect due to the stratigraphic position of the layer (i.e. to the depth of the layer). This index was calculated for both 1D and 2D numerical simulations according to equation (4).

$$\Delta\Gamma = SSCI - SSCI_{\text{hom}} \tag{4}$$

The distribution of the $\Delta\Gamma$ index versus the thickness of lithological unit 4 is reported in Fig. 5. It is worth noticing that the thickness is expressed by thickness classes and that the average value of the $\Delta\Gamma$ index for each class and their standard deviations are reported in Fig. 5.
Fig. 5 shows that the variability of the $\Delta\Gamma$ index is higher for thin layers (high values of standard deviation also in the case of a small number of data is available for the average) illustrating the strong influence of the vertical heterogeneities on the earthquake-induced strain levels. Such a trend is true for both 1D and 2D conditions.

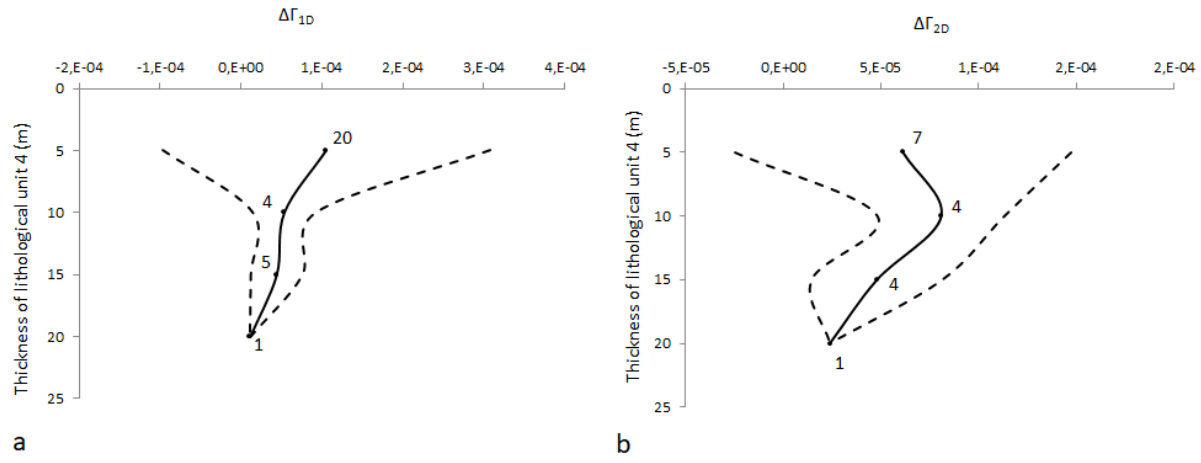

Figure 5. ΔΓ distributions vs. thickness of lithological unit 4 in 1D (a) and 2D (b) models. Black line indicates the average values; dotted lines indicate the computed standard deviations. The number of data available for computing the average is also shown in the plots.

The computation of ΔΓ was a preliminary step towards the evaluation of the role of the lateral heterogeneities, i.e. the role of the presence of a horizontal lateral impedance contrast, on the seismically induced strain. The $\Delta\Gamma_{1D\text{-}2D}$ index is a differential index obtained from the subtraction of the $\Delta\Gamma_{2D}$ from the corresponding $\Delta\Gamma_{1D}$ isolating the contribution of 2D effects on the seismically induced strain according to the following equation (5).

$$\Delta\Gamma_{1D-2D} = |SSCI_{1D} - SSCI_{2D}| \quad (5)$$

The so calculated $\Delta\Gamma_{1D\text{-}2D}$ index were correlated to the distance to the closest lateral heterogeneity characterized by a velocity contrast ΔV_S > 200 m/s including the seismic bedrock of the basin (Bard and Bouchon, 1985; Semblat et al., 2010) as well as the lateral heterogeneities within the alluvial fill (Martino et al., 2015).

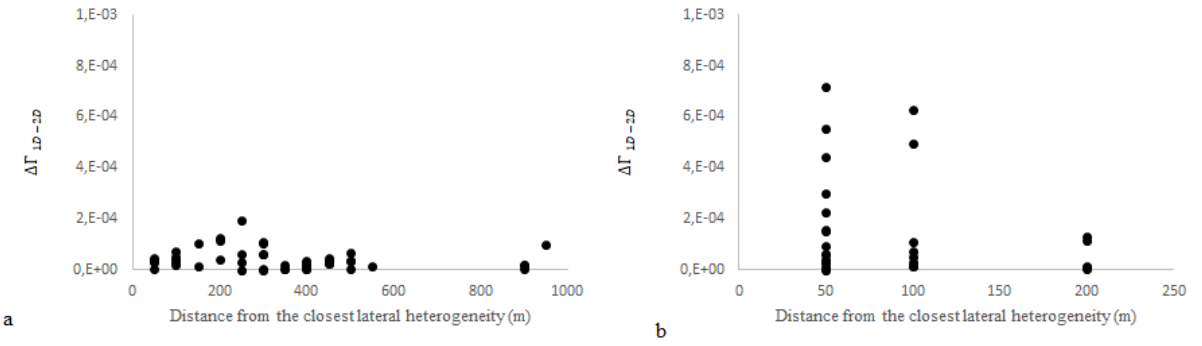

Figure 6. $\Delta\Gamma_{1D\text{-}2D}$ distributions vs. distance to the closest lateral heterogeneity characterized by a high-velocity contrast (ΔV_S > 200 m/s) for lithological units 2 (a) and 4 (b)

The analysis of the correlation between the $\Delta\Gamma_{1D\text{-}2D}$ and the closest lateral heterogeneity highlighted that some lithological units are more influenced by 2D effects (lithological unit 4 in Fig. 6b) while other lithologies (ex. lithological unit 2 in Fig. 6a) are not strongly affected by 2D effects because the $\Delta\Gamma_{1D\text{-}2D}$ varies around zero. In the first case, it is possible to notice a decreasing of the $\Delta\Gamma_{1D\text{-}2D}$ while the distance from the lateral heterogeneities increase (Fig; 6b) so indicating 2D effects strongly affecting the seismically-induced strain when impedance contrasts are closer than 100m. At the same time, the

example of lithological unit 2 (Fig. 6a) show no decreasing trend of $\Delta\Gamma_{1D\text{-}2D}$ with distance from the closest lateral heterogeneity so highlighting a weak role of 2D effect due to the lateral heterogeneities.

5. CONCLUSIONS

The Fosso di Vallerano alluvial valley (Rome, Italy) is characterized by a complex geological setting due to a high heterogeneity of the alluvial deposits as well as to an articulated shape of the seismic bedrock. Earthquake-induced shear strains and their concentrations were computed in terms of MMS, SSCI and $\Delta\Gamma_{1D\text{-}2D}$ indexes. The obtained MSS distributions output that shear strains are mainly concentrated in units 3 and 4 while there is a significant decrease in stiffer lithological units.
The analyzed $\Delta\Gamma_{1D}$ and $\Delta\Gamma_{2D}$ indexes highlighted a strong influence of vertical heterogeneities on the seismically induced strain. The obtained values of the $\Delta\Gamma_{1D\text{-}2D}$ index highlight that 2D effects influence the shear strain concentration within the softest lithological units. These preliminary results encourage further analysis to better explore the role of 2D effects on earthquake-induced shear strains due to the shape of the seismic bedrock and the heterogeneity of the alluvial deposits.

6. REFERENCES

Ascani F., Bozzano F., Buccellato A., Del Monte M., Matteucci R., Vergari F. (2008) - Evoluzione del paesaggio e antiche vie di drenaggio nell'area de "Il Castellaccio" (Roma) da indagini geologiche, geomorfologiche e archeologiche. In *Geologica Romana* 41. pp.55-77.

Bard P.-Y., Bouchon M. (1985) - The two dimensional resonance of sediment filled valleys. *Bull. Seism. Soc. Am.* 75. pp. 519–541.

Bardet J.P., Ichii K., Lin C.H.; (2000) - EERA. A computer program for Equivalent-linear Earthquake site Response Analyses of layered soil deposits. University of Southern California, Department of Civil Engineering, user's manual.

Bozzano F., Caserta A., Govoni A., Marra F. & Martino S. (2008)- Static and dynamic characterization of alluvial deposits in the Tiber River Valley: New data for assessing potential ground motion in the City of Rome. *Journal of Geophysical Research*, 113, B01303.

Bozzano F., Lenti L., Marra F., Martino S., Paciello A., Scarascia Mugnozza G., Varone C. (2016) - Seismic response of the geologically complex alluvial valley at the "Europarco Business Park" (Rome – Italy) through instrumental records and numerical modelling. *Italian Journal of Engineering Geology and Environment. 16(1),* pp. 37-55.

Caserta A., Martino S., Bozzano F., Govoni A., Marra F. (2012) - Dynamic properties of low velocity alluvial deposits influencing seismically-induced shear strains: the Grottaperfetta valley test-site (Rome, Italy). *Bull Earthquake Eng*, 10, pp. 1133-1162

Cundall, P., Hansteen, E., Lacasse, S., Selnes, P.B., (1980). NESSI, Soil Structure Interaction Program for Dynamic and Static Problems. Norges Geotekniske Institute, Norway (Report 51508-9).

Hardin, B. O., and V. P. Drnevich. (1972). "Shear Modulus and Damping in Soils: I. Measurement and Parameter Effects, II. Design Equations and Curves," Technical Reports UKY 27-70-CE 2 and 3,College of Engineering, University of Kentucky, Lexington, Kentucky. [These reports were later published in the Journal of Soil Mechanics and Foundation Division, ASCE, Vol. 98, No. 6, pp.603-624 and No. 7, pp. 667-691, in June and July 1972.]

ITASCA, (2011). "FLAC 7.0: User Manual", Licence Number SN 213–33-760- key 29753. IFSTTAR.

Kuhlemeyer, R.L., Lysmer, J., (1973). Finite element method accuracy for wave propagation problems. J. Soil Mech. Found. Eng. Div. ASCE 99 (SM5), 421–427.

Lysmer, J., and R. L. Kuhlemeyer. "Finite Dynamic Model for Infinite Media," J. Eng. Mech., (1969). 95(EM4), 859-877.

Martino S., Lenti L., Gelis C., Giacomi A.C., Santisi D'Avila P., Bonilla F., Bozzano F., Semblat J.F. (2015) . Influence of lateral heterogeneities on strong motion shear strains: simulations in the historical center of Rome (Italy). *BSSA, 105(5),* pp. 2604-2624.

Semblat J.F., Lokmane N., Driad-Lebeau L., Bonnet G. (2010) - Local amplification of deep mining induced

vibrations part 2: simulation of ground motion in a coal basin. *Soil Dyn Earthq Eng* 30(10). pp. 947–95

Varone C., Lenti L., Martino S. (2014). Engineering-geological and numerical modeling for the evaluation of the vibrational interaction between the city agglomerate and heterogeneous geological system: preliminary results. *Atti del 33° Convegno GNGTS, Bologna (Italy), v. 2 Caratterizzazione sismica del territorio.*